In situ magnetometry studies of magnetoelectric LSMO/PZT heterostructures

Philipp M. Leufke,[1,*] Robert Kruk,[1] Richard A. Brand,[1,2] and Horst Hahn[1,3]
[1]*Institute of Nanotechnology (INT), Karlsruhe Institute of Technology (KIT), Karlsruhe, Germany*
[2]*University of Duisburg-Essen, Germany*
[3]*KIT-TUD-Joint Research Laboratory Nanomaterials, Technische Universität Darmstadt, Germany*
(Received 29 December 2012; published 14 March 2013)

In order to identify and quantify characteristics of the magnetoelectric coupling at ferromagnetic/ferroelectric interfaces, epitaxial $La_{1-x}Sr_xMnO_3$/Pb(Zr,Ti)O_3 (LSMO/PZT) heterostructures were deposited by large-distance magnetron sputtering. The remarkably high lateral uniformity achieved in such films allowed for a ferroelectric device area of more than 6 mm^2. This has enabled for superconductive quantum interference device (SQUID) measurements of the magnetic response to the systematically, completely *in situ*, varied remanent ferroelectric polarization. Temperature dependence of the magnetic modulation upon charging and the magnetic response to the ferroelectric stimulation indicate a field-effect dominated coupling mechanism and generally confirm the concept of electrostatic hole (h^+) doping of LSMO. The modulation of magnetization was comprehensively analyzed for a broad range of electrostatically induced surface charge concentrations. For small charge modulations at low temperature a linear tuning coefficient of $\approx -3.6\ \mu_B/h^+$ has been determined. This suggests the activation of an antiferromagnetic coupling, even for very small surface charge densities. Simultaneously, a shift in the magnetic transition temperature at higher surface charge concentration indicates the presence of a ferromagnetic phase at the LSMO/PZT interface. Eventually, a physical picture of magnetoelectric coupling is proposed in which these quantitative results are consistently interpreted, in terms of a surface-charge dependent electronic phase separation with the coexistence of antiferromagnetic and ferromagnetic regions at the ferromagnetic/ferroelectric interface.

DOI: 10.1103/PhysRevB.87.094416 PACS number(s): 75.85.+t, 85.80.Jm, 77.55.Nv, 75.30.Kz

I. INTRODUCTION

There has been continuous interest in the electrostatic control of magnetism in $La_{1-x}Sr_xMnO_3$ (LSMO) and related perovskite manganites due to their strong correlation between the charge density (i.e., chemical hole doping level) and the magnetic and transport properties.[1–17] In recent years, an alternative approach to chemical hole (h^+) doping, the modulation of the surface carrier density by application of an electrostatic field (electrostatic doping), has been proposed and tested on several composite systems. While the electrostatic doping can be implemented by inducing surface charge with the help of the Helmholtz double layer of an electrolyte[17] or by amplifying the applied electric field with a high-κ dielectric,[7,12] the focus of ongoing research has been on combining LSMO with ferroelectrics (FE)—e.g., Pb(Zr,Ti)O_3 (PZT)—thus forming multiferroic heterostructures.[5,15]

The attraction of such artificial multiferroic thin film systems lies not only in the scarcity of single-compound multiferroics,[5] but also in their virtually unlimited tailorability through the choice of materials and doping levels and the resulting effects.

The majority of published studies cover the modulation of transport properties, mostly electrical resistance[1,3,4,6,13,18–20] but also magnetotransport[2,7,14] and multiferroic tunnel junctions.[14] The sheet resistance modulation (Mott transition) in a FE field-effect transistor (FE-FET) structure is comparatively easy to produce as it does not require large defect-free FE layers. Furthermore, some manganites are known to drastically decrease fatigue in Pb(Zr,Ti)O_3, making them natural candidates for robust FE-FETs.[21]

A modulation of the channel resistance by 300% was reported by Mathews *et al.*,[1] employing 30 to 50 nm thick $La_{0.7}Ca_{0.3}MnO_3$ (LCMO) channels. Pallecchi *et al.*[7] achieved an on-off ratio of 250% in a side-gated geometry with a 7 u.c. (unit cells) thin $La_{0.7}Sr_{0.3}MnO_3$ channel and $SrTiO_3$ (STO) as gate dielectric. An electrostatically induced shift of 43 K was observed in the metal-insulator transition temperature T_{MI}, similar to a 50 K shift reported by Hong *et al.*[4] In $La_{0.85}Ba_{0.15}MnO_3$ (LBMO), a shift of 1.5 K was achieved by Kanki *et al.*[3]—comparatively low, but in contrast to the aforementioned with the magnetic transition taking place around room temperature. They also demonstrated a mostly linear behavior of both the resistivity modulation and the shift in T_{MI} with respect to the remanent FE polarization. Later[6] the resistance modulation was shown to be accompanied by a modulation of the magnetization.

Apart from field-effect devices, strain mediated effects on the manganite layer have been demonstrated in which the crystal lattice is modulated through a phase transition[22] or the inverse piezoelectric effect[18–20,23] of the ferroelectric. The latter can only be observed when it is not outshined by the stronger field effect; this is achieved by choosing the manganite's doping level to be in a plateau region of the phase diagram (e.g., $x \approx 0.3$ for LSMO) and/or by increasing the film thickness, since the elastic strain is a long-range effect as opposed to the very short screening length of the electric field effect.

Besides any potential applications, the study of electrostatic tuning of magnetism in hole-doped manganites can lead to new insights into the fundamental physical mechanisms because of the absence of the extrinsic effects of distortion and disorder inherent in chemical doping. However, the investigation of magnetic effects in manganite/FE composite systems is a challenging task as it requires a setup which allows for polarization

of the FE and measuring the magnetization, preferably at variable external magnetic fields and temperatures.

On the one hand magneto-optical Kerr effect (MOKE) is commonly preferred for *in situ* charging experiments over the superconductive quantum interference device (SQUID) magnetometry[6,9–12]—despite possible side effects originating from the ferroelectric[24]—because the required size of the tuned area can be relatively small. On the other hand, as a SQUID provides a direct quantitative information, it is usually employed for calibration of the MOKE results on, presumably similar, reference samples.

Some of the most remarkable results on magnetic modulation of STO/$La_{0.8}Sr_{0.2}MnO_3$/$PbZr_{0.2}Ti_{0.8}O_3$ heterostructures were reported by Molegraaf, Vaz, and co-workers,[9–11] featuring a shift of the ferromagnetic (FM) Curie temperature T_C of 20 K and modulations of the magnetization of ≈20% with a change of the sign of the modulation at 150 K. After correlating the low-temperature relative change in magnetization and the surface charge density modulation ΔP_r, the pronounced tuning effect was attributed to the formation of an antiferromagnetic (AFM) phase which was theoretically predicted by Burton *et al.*[8] However, those *ab initio* calculations were based on a high doping level of $x = 0.5$ and fully strained $BaTiO_3$ (BTO) as top-gate FE and did not address the experimentally evident presence of a FM phase showing a pronounced shift in T_C.

Presumably in an attempt to attest this theory, Lu, Burton *et al.*[16] recently investigated FE tuning of BTO-gated LSMO with a relatively high doping level of $x = 0.33$ and thicknesses of 10 to 50 nm in a SQUID magnetometer; the necessary large FE device area was *ex situ* polarized employing a noncontact scanning probe tip, in order to avoid leakage current problems. While a 10% magnetic modulation in hole depletion mode was observed at room temperature, no evidence for the expected AFM coupling in accumulation mode was found. The large magnetic tuning effect was explained by a drastically increased screening length caused by a metal-to-insulator transition in the interfacial volume of the LSMO. It should be noted that for this heterostructure no shift in T_C and no crossover in the sign of the effect was found in the investigated temperature range.

The same LSMO chemical doping level was also studied by Brivio *et al.*,[12] employing top- and bottom-gating with STO thin films, where a shift in T_C of 5 K was found in a 3 nm thin LSMO film. In the course of studies an important observation was made that an effective magnetic modulation could only be achieved in top-gating geometry. The absence of the effect for the bottom-gating configuration was ascribed to a magnetically dead layer at the bottom LSMO interface of about 2 nm thickness.

The existence of magnetically dead layers is a well known fact for manganite perovskites[25–29] and their thickness was found to extend up to 2 to 5 nm, depending on the substrate. So far, in all reports on the successful modulation of magnetic or transport properties, the manganite layers have always been thicker than the minimal dead layer thickness. Despite the crucial role of the dead layer in the correct estimation of the total magnetization of the whole LSMO layer—and thus its impact on the *relative* amplitude of the Kerr signal—only few reports on manganite field effect devices mention or consider the dead layer existence[4,7,12] and none of the quantitative evaluations of the magnetic modulation account for it.

In this paper we present an approach to circumvent the uncertainty caused by the dead layer factor by directly correlating the absolute magnetic modulation with the *in situ* measured total remanent charge modulation ΔQ on the entire samples. Unlike MOKE, the SQUID magnetometry can directly deliver quantitative magnetization data with unrivaled accuracy and sensitivity. Provided that the space charge region is not disturbed by the dead layer—i.e., the investigated LSMO layer is thicker than the maximum dead layer thickness plus the expected screening length,[8] 5 nm + 3 u.c. ≈ 6.2 nm < d_{LSMO}—and assuming that each FE remanent charge is screened by mobile charges in the LSMO layer,[10] the magnetic modulation per charge can be monitored directly.

A practical challenge for *in situ* charging experiments lies in the requirements for the lateral size of the field-effect device. Since the electrostatic doping is an interface effect, a relatively large device area of several square millimeters is necessary to deliver a significant signal-to-noise ratio.[30] This demanding lateral homogeneity of the FE thin films with complete absence of fatal pinholes over a large area has been accomplished by large-distance magnetron sputtering.[31]

In the following we will present LSMO/PZT heterostructures whose characteristics prove the charge modulation as the sole cause for the magnetization modulation and show that any contribution of inverse piezoelectric nature can safely be neglected.

By comparing quantitative SQUID data with the results of Molegraaf, Vaz *et al.*,[9–11] the role of a magnetically dead layer will be critically discussed. Eventually, we will investigate the dependence of the magnetic modulation on temperature, the induced charge modulation, and the shape of the field cooling (FC) curve, which will lead to further insight into the interplay of AFM and FM coupling in this electrostatically controlled interface.

II. EXPERIMENTAL DETAILS

In order to achieve high lateral uniformity, large-distance rf-magnetron sputtering was employed to deposit the $La_{0.87}Sr_{0.13}MnO_3$ and $PbZr_{0.52}Ti_{0.48}O_3$ thin films onto epi-polished, (100)-oriented, conductive $SrTiO_3$:Nb (STO:Nb) as described elsewhere.[29,31] On the one hand a reduction in LSMO film thickness results in reduction of transition temperatures, but on the other hand it increases the relative magnetic modulation by increasing the ratio of tuned to untuned volume. Thus a thickness of 7.2 nm was found to provide a good compromise; the film was also thick enough not to be affected by the dead layer. For the PZT layer 90 nm thickness was chosen, being thick enough to be pinhole-free over large areas and thin enough to be—even at low temperature—fully polarizable in the voltage range of the ferroelectric tester (±10 V). A reduced PZT film thickness also helped reduce the inverse piezoelectric effect by decreasing the—for the 52/48 PZT composition otherwise relatively high—piezoelectric coefficient[32,33] which could induce magnetostrictive coupling in the LSMO layer.[20]

An array of 1×1 mm^2 large Au top electrodes of 25 nm thickness was deposited through a shadow mask by dc sputtering. Then each of the FE capacitor devices was tested and the device area was measured in an optical microscope.

Reciprocating sample option (RSO) SQUID measurements in an in-plane geometry were carried out in a Quantum Design MPMS *XL* magnetometer which was accordingly modified to allow for attaching up to four independent electrical connections. To avoid any spurious signal, solely diamagnetic materials were chosen for contacting of the samples. The sample was bonded to a Cu backing plate which was used as a bottom electrode and the triaged FE devices were bundled into two sets, where each one was addressed with a separate Kapton-coated Cu wire. All Cu parts were designed to extend uniformly along the whole sample space (i.e., beyond the RSO scan range). Conductive carbon and silver epoxies, which were tested for low-temperature SQUID measurements, were employed for bonding of the top and bottom contacts. The role of the Cu backing plate was twofold: first it served as a bottom electrode, but it also acted as an effective heat sink for possible Ohmic heating, keeping the sample in thermal equilibrium. In fact, during the successive RSO measurements, no temperature-drift induced signal modulation was detected at any time.

The ferroelectric measurements were carried out with a Radiant RT66B tester. Due to the considerable device area of the combined sets ($2.2\ \text{mm}^2 + 3.9\ \text{mm}^2 = 6.1\ \text{mm}^2$), which means large electrical capacity, and the comparatively high resistance of the STO:Nb substrate, the sample required longer voltage sweeping periods of around 200 to 400 ms to reach polarization saturation. Especially at low temperature, the parameters needed to be adjusted towards higher voltage and cycle time to compensate for the increased FE coercivity.[34,35]

For a number of reasons, all magnetic modulation measurements were deliberately performed in FE remanence mode: First of all, the SQUID magnetometry is slow (20 s per data point) in comparison to the MOKE one, and a high dc-bias voltage applied for longer times would result in degradation, Ohmic heating, and ultimately in TDDB (time-dependent dielectric breakdown) of the PZT thin film.[36] Secondly, if due to the degradation processes the overall leakage current rises to about 1 μA, the ensuing current loop can become detectable and distort the actual measurements. Thirdly, the actually applied charge at the LSMO/PZT interface cannot be reliably determined for statically biased devices, as the real charging current cannot be distinguished from the leakage currents. On top of that, the continuous application of static or periodic bias fields could not only induce thermal effects but also chemically alter the LSMO layer through the migration of oxygen vacancies into the oxide electrode.[21,37] Using dynamic FE hysteresis measurements for calibration is also not sufficient to adequately determine the saturation polarization due to its inherent vulnerability to frequency-dependent artifacts.[38,39] In summary, the remanent polarization of a ferroelectric is much better defined and can be determined by subtraction of the integrated charge of a nonswitching pulse and a switching pulse ("positive up, negative down", PUND[39]).

In the present experiment, repetitive RSO measurements were performed in between the triangular PUND test impulses, which were utilized to polarize the PZT and calculate the actual charge accumulated on the whole sample. Analogously, the total magnetic modulation was then calculated as the difference of the magnetizations for opposite FE polarization states.

The benefit from observing only the difference signal is that all unaffected magnetic moments—from untuned LSMO volume and possible spurious contributions from the contacting setup—are automatically canceled out. As this is an absolute measurement, the thickness of the dead layer is also irrelevant as long as the film is thick enough to accommodate the dead layer plus the full screening length. The magnetization modulation measurements were usually performed at relatively low fields of 100 to 200 Oe, below FM saturation, so as to avoid field induced distribution of the magnetic transition temperatures. The other concern was that high magnetic fields could introduce adverse side effects on the charging behavior of the FE devices due to the modulation of the magnetoresistance of the LSMO bottom electrode.[40]

It should be noted that in the present setup—differently from the usual FET nomenclature—the positive electrode was connected to the bottom contact and the negative one to the top-gate contact. This assignment was chosen because the drive electrode of the FE tester is recommended to be placed on the common bottom electrode in order to reduce noise pickup. Besides, this way the sign of the applied voltage corresponds the induced screening charge in the LSMO layer, which can directly be interpreted as hole accumulation and depletion, respectively.[17]

III. RESULTS

As the details of the structural, compositional, magnetic and FE characteristics are described in depth elsewhere,[29,31] we will only recapitulate the main points of these studies.

Due to the low lattice misfit and low film thickness, the LSMO layer grows commensurately on the cubic STO:Nb substrate in a tetragonal structure. In contrast, despite an atomically smooth LSMO/PZT interface, the PZT film shows fully strained growth only in the first two monolayers, followed by a roughly 5 nm thin relaxation region which effectively accommodates the large lattice mismatch. Beyond this region, the PZT film again becomes single-crystalline throughout the entire film thickness.

Despite the low Sr doping level ($x = 0.12$) of the LSMO film under consideration, the Curie temperature is significantly higher than in the bulk counterpart[41,42] (see T_C in Fig. 1)—a known phenomenon for low-doped manganite thin films, commonly attributed to fully strained growth below the relaxation threshold thickness.[43–45] It is important to note that the tested thin films were both ferromagnetic and electrically conducting as expected in double exchange mediated magnetism.[29]

The temperature dependence of the magnetic modulation upon charging and the corresponding FC curve are shown in Fig. 1. In order to avoid any assumptions about the dead layer (FC curve, M) and the screening length (magnetic modulation curve, ΔM), both curves are merely normalized on the unit cell areas (u.c.^{2}), accounting for the entire LSMO sample area in the first case and for the FE device area in the latter case. For the modulation measurement the FE charge density modulation was kept at $\Delta P_r \approx 20\ \mu\text{C/cm}^2$ ($0.19\ h^+/\text{u.c.}^2$), which required an adjustment of the FE cycle time to compensate for the temperature drift of the FE switching process. An unchanged magnetic modulation after

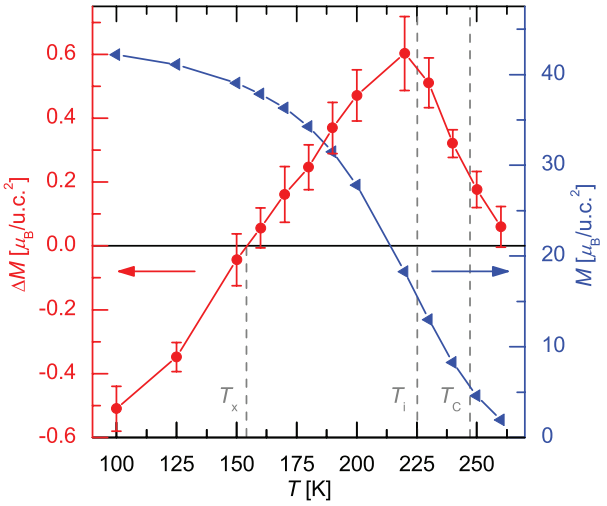

FIG. 1. (Color online) Temperature dependence of the magnetic moment and the magnetization modulation per unit cell area for a remanent charge modulation of 20 μC/cm^2 measured at an external field of 200 Oe. T_C, T_i, and T_x indicate the Curie temperature (247 K, as determined by Arrott's method[46]), the inflection point of the FC curve, and the crossover point of the magnetic modulation, respectively.

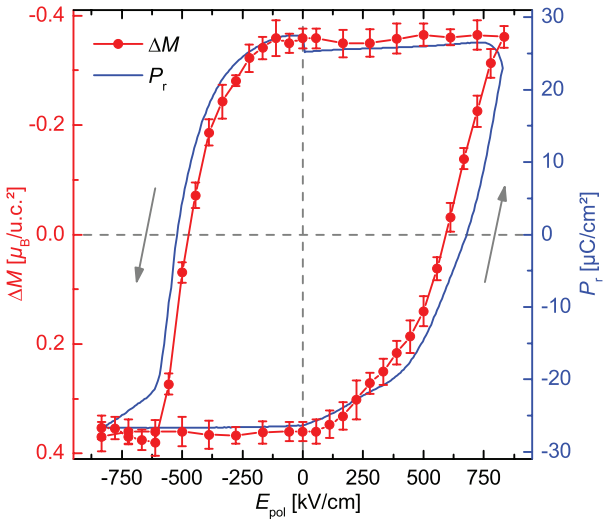

FIG. 2. (Color online) Comparison of the FE remanent hysteresis P_r and the response of the magnetic modulation ΔM per unit cell area. Both curves measured consecutively at 50 K and 100 Oe.

one day confirmed the previously assessed good FE retention of the PZT thin films.[31]

This particular measurement, and the ones shown in Fig. 3, were performed on a reduced device area (2.2 mm^2); thus the statistical error is larger. For all presented measurements where no error bars are shown, the statistical errors are smaller than the symbol sizes.

The magnetic modulation, i.e., the difference of the magnetizations in hole accumulation and depletion state, $\Delta M = M_{acc} - M_{depl}$, follows the temperature behavior which is expected for low-doped LSMO.[11,17] There are three distinctive regimes[9] with a local maximum around the point of inflection of the FC curve, a crossover of the tuning effect at T_x, and a reversed sign at lower temperatures.

In order to verify the magnetic tuning effect, the external magnetic field was also reversed, resulting in an expected reversal of the modulation. Also by varying the number of simultaneously polarized sets of FE devices it could be shown that the magnitude of the modulation scales with the device area.

Figure 2 illustrates the response of the magnetization to the polarization switching of the PZT film and the remanent FE hysteresis for comparison.[47] The remanent FE hysteresis loop was obtained by means of a PUND test with triangular voltage pulses, which allows for subtracting the nonswitching current components.[48] For the magnetic measurement successively stepped triangular voltage pulses were applied and the magnetic moment of the sample was recorded in the intervals between the pulses. The discrepancy in coercivity and saturation behavior originates from the difference in the time constants of both experiments—for the magnetic modulation curve the electric field for each data point was set by a 200 ms monopolar triangular pulse, while the same pulse duration was used for the full bipolar FE hysteresis.

An essential outcome of this experiment is the fact that both curves are strikingly similar, evidencing a purely electrostatic coupling mechanism with negligible piezoelectric influence. The lack of the piezoelectric effect is actually expected from the fact that the measurements are carried out only in FE remanence mode, which does not distinguish remanent ferroelastic strain states of the *c*-oriented tetragonal PZT.[49] Furthermore, the apparent absence of any butterfly shaped contribution to the magnetic response loop evidences the insignificance of possible strain-driven contributions caused either by the varying number of 180° FE domain walls for different remanent states of the single-crystalline PZT or by the existence of differently oriented PZT grains in the 5 nm thick relaxation region at the LSMO/PZT interface.

The temperature dependence of the magnetic response to the remanent FE hysteresis is illustrated in Fig. 3. The two hystereses represent the switching behavior at the negative and positive regimes of the tuning effect within the temperature range investigated in Fig. 1. The difference in coercivities is caused by the temperature dependence of the PZT characteristics and the FE imprint shift induced by the electrode configuration.[31]

In order to methodically investigate the change in magnetization as a function of the charge modulation ΔQ, the magnetization was recorded for a series of decreasing PUND polarization voltages U_{pol} at temperatures well below T_C. As Fig. 4(a) (and Fig. 2) illustrates, the magnetic signal shows very low noise fluctuations and high stability over time. The repetition of the maximum 7.5 V cycle at the end of the sequence confirmed the reproducibility of the charging process. The asymmetry in the decay of the modulation amplitude for positive and negative charging could be ascribed to the previously recorded characteristics of charging currents; the positive half of the FE polarization hysteresis required higher field (or longer time) to reach saturation while the negative side saturated at rather low fields (compare Fig. 2 and Ref. 31). Unfortunately, charging asymmetry cannot be discerned by the common current integration measurements,

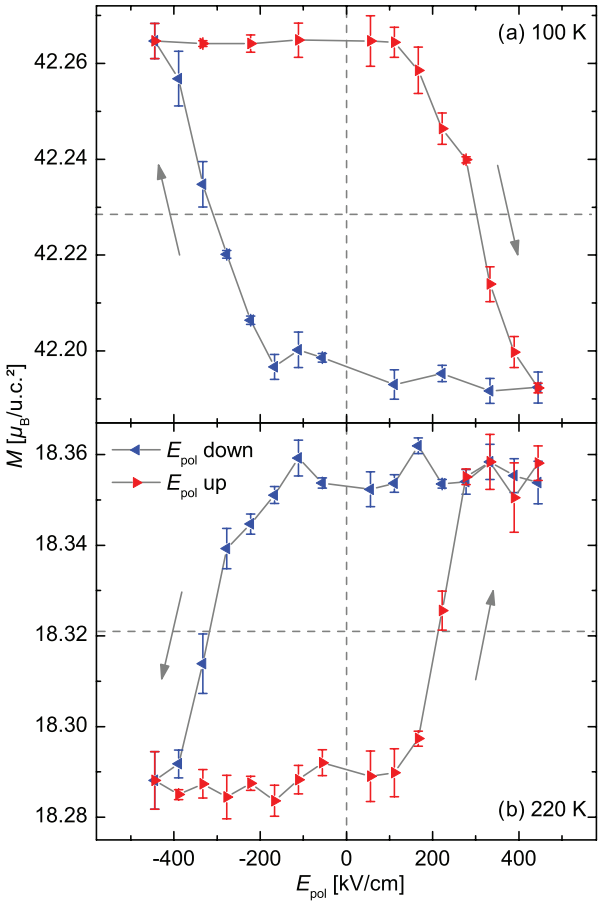

FIG. 3. (Color online) Temperature dependence of the magnetic response to the FE remanent hysteresis, measured at an external field of 200 Oe, below (a) and above (b) the crossover temperature T_x. The dashed crosshairs are guides to the eye.

because the constant of integration is not known. Although an asymmetric magnetic response of the LSMO to the FE charging cannot be excluded, the relative change of the polarization, however, is well defined.

Figure 4(b) shows the absolute magnetic modulation as a function of ΔQ as derived from the PUND tests performed in between the magnetic measurements; the 100 Oe curve corresponds to the raw data shown in Fig. 4(a). In order to investigate the magnetic field dependence at ± 7.5 V, the magnetic modulation was also measured for various fields up to FM saturation. The dashed curve was calculated by scaling the 100 Oe measurement to the value at 2 KOe as a good estimate for the tuning behavior for saturated magnetization.

IV. DISCUSSION

The complexity of a system like LSMO and its response to electrostatic charging require a cautious discussion. So far, the only sources of experimentally established information that are commonly used for discussing electrostatic doping phenomena are the LSMO bulk phase diagrams (for example Ref. 42), especially when considering temperature-dependent relationships.[2,10,12,16,19] Albeit in many instances this may lead to valid conclusions, the following constraints should always be kept in mind:

(1) The magnetic properties of the perovskite manganites strongly depend upon the Mn-O-Mn bond angle which may be affected by the chemical inhomogeneity and crystal lattice distortions that are introduced by chemical doping; yet these effects are absent in field-effect devices.

(2) While the chemically doped compound remains electrically neutral for all Sr compositions, the electrostatically doped interface is subjected to a very strong local electrostatic field.

(3) The bulk phase diagram may not be applicable when interface or strain effects come into play; magnetically dead layers and strain induced shifts in transition temperatures are some of the striking examples.

The noticeable scatter of characteristics and magnitudes of electrostatic tuning effects in LSMO and related compounds reported in literature emphasizes evident difficulties in correct interpretation of the underlying physical phenomena. While

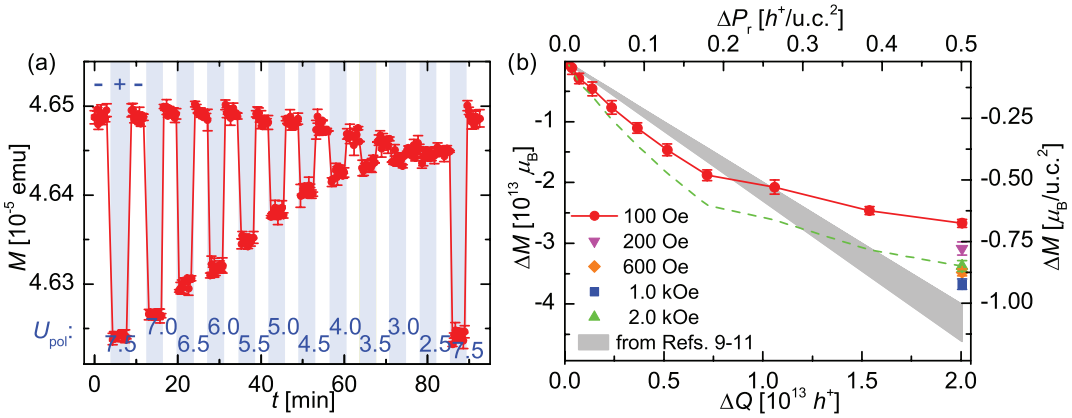

FIG. 4. (Color online) Dependence of the magnetic modulation on the induced charge modulation at 50 K. (a) Raw data illustrating modulation of sample magnetization at an external field of 100 Oe with the measurements recorded in remanent FE polarization after polarizing as indicated by U_{pol} and the shaded background. (b) Magnetic vs charge modulation ΔQ both of the whole sample and normalized on the LSMO unit cell area, respectively. The 100 Oe curve corresponds to the raw data in (a); other fields are shown for comparison; the dashed line visualizes the 100 Oe curve scaled to the saturation moment at 2 KOe. The gray shaded area marks the tuning efficiency as estimated from Refs. 9–11.

there have been attempts to theoretically predict the response of a manganite to the FE polarization for certain doping levels,[8,50] there is no general description available to account for the aforementioned complexities. Of course, eventually, it is also possible that entirely new electronic phases can be formed by field-effect tuning, which are not covered in the bulk phase diagrams at all.

The first essential observation concerns the magnetic modulation versus ΔQ at low temperatures: a direct coupling of the FE polarization and the magnetic response is apparent (see Fig. 2), with the induced change in magnetization closely following the FE polarization. The same applies to the similar measurements performed around T_C [see Fig. 3(b)], which qualitatively differ in the sign of the modulation only, as expected.[11]

A closer look at the actual charge dependence of the magnetic modulation reveals the nonlinearity in the trend above certain FE polarization threshold. When rescaled to the saturated magnetization [Fig. 4(b), dashed line], a steeper slope for $\Delta P_r < 0.2\ h^+/\text{u.c.}^2$ can be linearly approximated, giving a tuning coefficient equivalent to the total change of the magnetic moment of one Mn atom ($\alpha \approx -3.6\ \mu_B/h^+$).

Having estimated tuning coefficients, we make a small digression to put our quantitative results into the context of the reports by Molegraaf *et al.*[9] and the follow-up by Vaz *et al.*,[10,11] as they explored in their works similar physical aspects with different experimental tools, i.e., MOKE magnetometry. The foremost problem in quantification of MOKE measurements stems from the need for an external calibration, as MOKE can only provide relative values. Thus, for instance, a dead layer at the LSMO bottom interface can drastically change the estimated magnetic moment when averaged over the full film thickness instead of considering only the magnetically active part. The unusually low saturation magnetization of 0.9 μ_B/Mn reported in Ref. 9 is a strong indication for such a dead layer. Interestingly, such a supposition is backed by the measurements reported elsewhere.[51,52] Consequently, assuming a magnetic moment of 3.3 to 3.6 μ_B/Mn—as the nominal bulk value of 3.8 μ_B/Mn typically is not reached in thin films—the dead layer would come to be about 2.9 to 3.0 nm, a rather credible value. Thus, the tuning coefficient, corrected for the dead layer $\alpha = \Delta M/\Delta Q$, would be of $-2.3\mu_B/h^+$ to $-2.1\ \mu_B/h^+$. For better comparison, the corresponding slopes are indicated by the gray shaded area in Fig, 4; the actual single data points would be located beyond the axis ranges. It becomes evident from this illustration that, to a great extent, we can reconcile results obtained by Molegraaf *et al.*[9] with our experimental values just by the sensible assumption of a dead layer in their sample. Of course, at this point, one should bear in mind that the above considerations about the implications of the dead layer presence are hypothetical and must be tested by an independent experiment. Also other factors, such as preparation methods or differences in the doping level, are not accounted for in our speculations.

In the context of the previous studies, we think that the actual significance of the results presented here rests in their comprehensiveness; i.e., the magnetic modulation upon charging is tracked down continuously from virtually zero to the experimentally attainable maximum charge concentration.

A tentative examination of the magnetic response to the surface charge brings attention to two facts: First, for small ΔP_r the dependence is simply linear, but right from the start has a high slope (tuning coefficient) of $\alpha \approx -3.6\ \mu_B/h^+$. Second, no evidence for any *abrupt* phase transition upon charging is found. In principle, the charging experiments carried out at low temperatures were meant to extract contributions to the magnetic modulation unaffected by the critical effects at the magnetic transition temperature. If the interface magnetism were determined by pure double exchange mechanism only, one would expect to get a tuning coefficient equal to -1. This is a consequence of a simple fact that one electrostatically introduced hole is equivalent to the loss of one electron, carrying a magnetic moment of 1 μ_B. The absolute value determined in the present study is much bigger, and the actual value of $-3.6\ \mu_B$ suggests that, on average, one electrostatically introduced hole annihilates a whole Mn magnetic moment. The most plausible scenario accounting for the apparent disappearance of the entire Mn moment is the presence of AFM coupling[53] even for very low electrostatic hole doping levels. It looks like the AFM phase starts to form

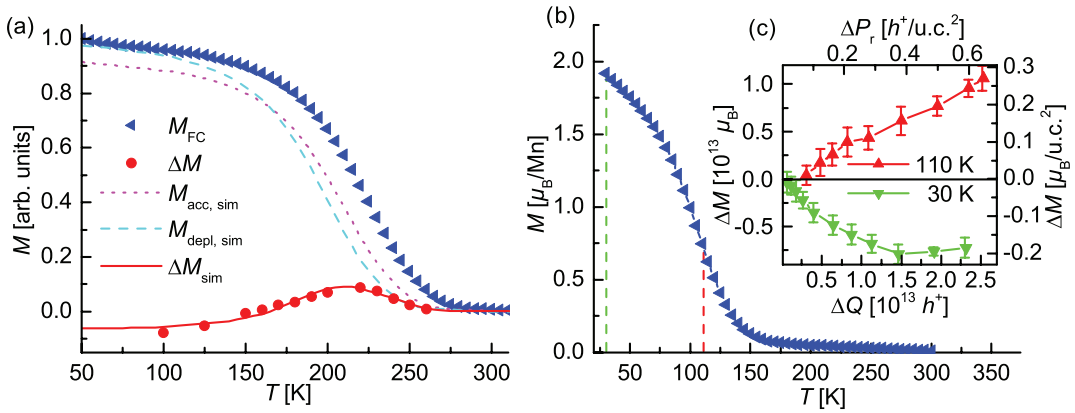

FIG. 5. (Color online) (a) Simulation of the temperature dependence of the tuning effect (compare Fig. 1). (b), (c) Low-T_C sample with 5 nm LSMO layer: FC measurement illustrating the smeared-out transition (b) and its effect on the tuning efficiency below and above the crossover temperature at 30 and 110 K, respectively (c). The measurements were performed at an external field of 100 Oe.

right away from the beginning of the charging process, and with increasing surface charge density covers more and more of the LSMO/PZT interface. The space expansion of the AFM phase over the interface area is a continuous process as can be seen in Fig. 4(b). The growth of the AFM phase dominates the magnetization modulation for charge densities below $0.2\,h^+/\text{u.c.}^2$ For higher ΔP_r, the tuning coefficient α gradually becomes smaller, signaling that induced antiferromagnetism is not the sole contributor to the tuning effect.

The change of tuning slope can be better explained by considering the overall temperature dependence of the tuning effect (Fig. 1). Phenomenologically, the resultant accumulation and depletion FC curves can be reconstructed from the magnetic modulation by scaling the magnetic moment in the untuned FC curve and then accordingly shifting it back and forth along the temperature axis.[9] Taking the untuned FC curve of the entire sample as a starting point, the shifts in T_C for the hole accumulation and depletion states can be numerically fitted to the experimentally determined temperature dependence of the magnetic modulation, as shown in Fig. 5(a). With a screening length of 2 u.c. and a dead layer thickness of 2.1 nm, the relative magnetization change between the FE polarization states amounts to about 7%. The transition temperatures are shifted by -14 and -24 K for the accumulation and the depletion state, respectively, resulting in a charge modulated shift of T_C by 10 K. The fact that *both* charged states are shifted to lower temperatures, with respect to the FC curve of the entire sample—representing a superposition of the distribution of the temperature dependence throughout the LSMO thickness—indicates that the T_C of the topmost layers is reduced, compared to the interior of the LSMO film.

While an AFM coupling may explain the pronounced (negative) tuning effect at low temperatures, it cannot account for the shift in T_C, which gives rise to the local (positive) maximum of the tuning effect around the point of inflection (T_i). As has already been pointed out, the magnetic modulation curve, with increasing temperature, passes a crossover point where the tuning effect changes sign from negative to positive. From the above analysis it is evident that the positive tuning effect around the transition temperature is a straightforward result of the shift in T_C upon charging. Indeed, on the basis of the bulk phase diagram[42] in the low-doping region, the shift suggests the presence of a ferromagnetically ordered component, which would require merely a minor charge modulation of less than $0.02\ h^+/\text{Mn}$ to yield a shift of more than 30 K.

The clear indication of the charge-induced AFM phase at low temperatures and the FM phase around T_C, together with the continuous temperature dependence of the tuning effect with no sign of any abrupt transitions (Fig. 1 and Ref. 11) suggest that AFM and FM coupling are likely to coexist over the whole temperature range, thus pointing to an electronic phase separation at the LSMO/PZT interface.

Assuming a physical model of the coexisting AFM and FM states, we set out to interpret the nonlinearity of the charge dependence (Fig. 4), again calling upon the notion of the transformation of the primary FC curve upon charging. Both the reduction of magnetic moment and the shift towards higher transition temperatures, when switching from the depletion to accumulation state, are a function of the applied ΔP_r. Although, in principle, both the effects can happen simultaneously, the change in magnetic moment dominates at low temperatures while the shift in transition temperature is naturally pronounced around T_C. However, at sufficiently high charge density, the charge dependence of the tuning effect at low temperature gets also influenced by the temperature shift as long as the FC curve is not perfectly leveled off in the respective temperature range. The evident impact of the shape of the FC curve is demonstrated in Figs. 5(b) and 5(c), where the smeared-out transition of a 5 nm LSMO sample causes the magnitude of magnetic modulation at 30 K to level off and then even decrease at higher ΔP_r.

The charge dependence at 110 K, around the point of inflection of the FC curve [Fig. 5(c)], gives even more insight into the magnetoelectric mechanisms. While showing a nearly linear dependence of the magnetic modulation with respect to the applied ΔP_r, there is a threshold below which no magnetic tuning could be determined with our experimental accuracy; a behavior which is in strong contrast to the one observed at low temperature. This can be understood by preferential inducement of the AFM coupling for low ΔP_r, presumably within the regions of the nucleating and forming FE domains. In these FE domains the local surface charge density would be high enough to trigger AFM interactions, which are difficult to detect around the transition temperature. Only at higher surface charge concentrations does the FM coupling take over the tuning effect.

Coming back to our original heterostructure (Fig. 4), the steep slope—i.e., the high tuning coefficient—at low temperatures and low ΔP_r can be understood as a direct consequence of a pure AFM coupling arising from the regions with higher local charge density. Such an inhomogeneous surface charge distribution at the LSMO/PZT interface could be quite naturally imagined during the FE polarization. For instance the regions of enhanced surface charge density would be connected to the process of formation of FE domains. As we have already stated, the increase in T_C has notable impact on the tuning coefficient even at low temperatures because the FC curve does not saturate (i.e., level off). Therefore, upon further charging the reduction of the absolute value of the tuning coefficient is caused by the competition between continuous growth of AFM ordered regions and increase of the T_C shift of the FM phase.

In essence, the explanation of the tuning effects rests in the fundamental fact that the competition of super-exchange, double-exchange, and electron-lattice couplings results in a staggering variety of possible phase states in mixed-valent manganites. Both our suppositions, i.e., the appearance of the AFM phase and its coexistence with the FM phase upon electrostatic hole accumulation, have already found positive support in some theoretical and experimental works. For example, in a recent article by Chen *et al.*[54] it is clearly shown from first-principle studies that for the LSMO/PZT, with nominal Sr doping level of $x = 0.2$, the accumulated holes do change the magnetic state of the interfacial manganite from FM to AFM. It should be noticed that this theory and the others dealing with the field-effect driven phase transitions in manganites either do not or cannot account for the *insulating* AFM phase in the hole depletion regime which is present in the bulk phase diagram. Indeed, as a matter of fact, our

experimental data also does not show any clear indication of an existence of antiferromagnetism in the hole depletion regime.

The proposed scenario of the electrostatically induced coexistence of the AFM and FM phases is compellingly backed by the well known phenomenon of spacial electronic phase separation in otherwise chemically homogeneous manganites.[55] Some experimental evidence of the AFM/FM phase separation at a manganite/FE interface one can find, for example, in work by Alberca *et al*.[56] In this article electronic transport and magnetic properties studies on epitaxial $La_{0.7}Ca_{0.3}MnO_3/BaTiO_3$ films suggest either phase separation between the AFM and FM local order, or alternatively a coexistence of in-plane and out-of-plane FM regions. Ultimately, to decide between these scenarios will require a series of *in situ* charging experiments with the sample oriented parallel and perpendicular to the applied magnetic field.

Another aspect that is not directly addressed in our studies is the dependence of the FE charging effect on the presence of ferromagnetic domains. For reasons we have stated in the experimental chapter, our experiments were carried out in a magnetically unsaturated state. However, at least at low temperatures, one should not expect much of a change in the tuning mechanism of the FM phase between magnetically unsaturated and saturated states. In principle, the tuning effect should be the same for all the FM domains so its net value should scale with the total magnetization. Of course, sensitivity of the AFM phase formation to the external magnetic field is much more difficult to predict and would require further experimental verification.

V. SUMMARY

We have made highly uniform multiferroic LSMO/PZT heterostructures, which provide sufficiently large FE device areas to allow us to simultaneously measure charge and absolute magnetic modulation using *in situ* SQUID magnetometry. Consequently, we report on the charge-dependent measurements of the magnetic response, carried out in the FE remanence mode, covering the physically relevant range of the surface charge modulation. An appropriate LSMO film thickness was chosen, not only to secure a higher T_C and a sharper magnetic transition, but also to ensure that the magnetically dead layer does not Interfere with the screening depth of the field-effect device. By considering only the differential magnetic signal and the total FE-induced remanent charge modulation ΔQ, possible spurious effects of both magnetic and ferroelectric origin were eliminated.

The remanent FE hysteresis and the system's magnetic response closely follow each other, evidencing practical absence of the inverse piezoelectric effect in this system in accordance with the microstructural analysis. The quantitative correlation of the total magnetic modulation and the charge modulation, normalized to the unit cell area, provides a charge-dependent tuning coefficient $\alpha = \Delta M/\Delta Q$. Its strikingly large value of $\approx -3.6\ \mu_B/h^+$, obtained at temperatures well below T_C, along with the in-depth analysis of the temperature- and charge-dependent modulation of magnetism, leads to the physical picture of the anti- and ferromagnetically ordered phases coexisting at the LSMO/PZT interface. While the antiferromagnetism is present even for very small charge density modulations, the FM response seems to require overcoming a certain threshold to be detectable. In this scenario it is very plausible that an inhomogeneous distribution of surface charge density, related to the formation of the FE domains, can naturally favor the spatial separation of the AFM and FM phases.

Furthermore, the charge-dependent tuning coefficient $\alpha = \Delta M/\Delta Q$, which is independent of *a priori* assumptions about the existence of a dead layer or the charge distribution within the screening length, can be used as a valuable starting point for further theoretical studies and modeling.

ACKNOWLEDGMENTS

We would like to thank Ajay Kumar Mishra and Di Wang from KIT for cooperation and fruitful discussions. This work was partially supported by the Deutsche Forschungsgemeinschaft (DFG) under Contract No. HA1344/28-1. The authors acknowledge support from the KNMF Laboratory for Spectroscopy and Microscopy and the State of Hessen for an equipment grant.

*leufke@kit.edu

[1] S. Mathews, Science **276**, 238 (1997).
[2] X. Hong, A. Posadas, A. Lin, and C. H. Ahn, Phys. Rev. B **68**, 134415 (2003).
[3] T. Kanki, Y.-G. Park, H. Tanaka, and T. Kawai, Appl. Phys. Lett. **83**, 4860 (2003).
[4] X. Hong, A. Posadas, and C. H. Ahn, Appl. Phys. Lett. **86**, 142501 (2005).
[5] W. Eerenstein, N. D. Mathur, and J. F. Scott, Nature (London) **442**, 759 (2006).
[6] T. Kanki, H. Tanaka, and T. Kawai, Appl. Phys. Lett. **89**, 242506 (2006).
[7] I. Pallecchi, L. Pellegrino, E. Bellingeri, A. S. Siri, D. Marré, A. Tebano, and G. Balestrino, Phys. Rev. B **78**, 024411 (2008).
[8] J. D. Burton and E. Y. Tsymbal, Phys. Rev. B **80**, 174406 (2009).
[9] H. J. A. Molegraaf, J. Hoffman, C. A. F. Vaz, S. Gariglio, D. van der Marel, C. H. Ahn, and J.-M. Triscone, Adv. Mater. **21**, 3470 (2009).
[10] C. A. F. Vaz, J. Hoffman, Y. Segal, J. W. Reiner, R. D. Grober, Z. Zhang, C. H. Ahn, and F. J. Walker, Phys. Rev. Lett. **104**, 127202 (2010).
[11] C. A. F. Vaz, Y. Segal, J. Hoffman, R. D. Grober, F. J. Walker, and C. H. Ahn, Appl. Phys. Lett. **97**, 042506 (2010).
[12] S. Brivio, M. Cantoni, D. Petti, and R. Bertacco, J. Appl. Phys. **108**, 113906 (2010).
[13] J. Hoffman, X. Hong, and C. H. Ahn, Nanotechnology **22**, 254014 (2011).
[14] Y. W. Yin, M. Raju, W. J. Hu, X. J. Weng, X. G. Li, and Q. Li, J. Appl. Phys. **109**, 07D915 (2011).
[15] C. A. F. Vaz, J. Phys.: Condens. Matter **24**, 333201 (2012).

[16]H. Lu, T. A. George, Y. Wang, I. Ketsman, J. D. Burton, C.-W. Bark, S. Ryu, D. J. Kim, J. Wang, C. Binek, P. A. Dowben, A. Sokolov, C.-B. Eom, E. Y. Tsymbal, and A. Gruverman, Appl. Phys. Lett. **100**, 232904 (2012).
[17]A. K. Mishra, A. J. Darbandi, P. M. Leufke, R. Kruk, and H. Hahn, J. Appl. Phys. **113**, 033913 (2013).
[18]C. Thiele, K. Dorr, L. Schultz, E. Beyreuther, and W.-M. Lin, Appl. Phys. Lett. **87**, 162512 (2005).
[19]C. Thiele, K. Dörr, W.-M. Lin, K.-H. Müller, and L. Schultz, Sensors and Actuators A **129**, 180 (2006).
[20]K. Dörr and C. Thiele, Phys. Status Solidi B **243**, 21 (2006).
[21]F. Chen, Q. Z. Liu, H. F. Wang, F. H. Zhang, and W. Wu, Appl. Phys. Lett. **90**, 192907 (2007).
[22]W. Eerenstein, M. Wiora, J. L. Prieto, J. F. Scott, and N. D. Mathur, Nat. Mater. **6**, 348 (2007).
[23]R. K. Zheng, Y. Wang, H. L. W. Chan, C. L. Choy, and H. S. Luo, Appl. Phys. Lett. **90**, 152904 (2007).
[24]I. E. Chupis, Low Temp. Phys. **23**, 213 (1997).
[25]J. Z. Sun, D. W. Abraham, R. A. Rao, and C. B. Eom, Appl. Phys. Lett. **74**, 3017 (1999).
[26]K.-H. Müller, K. Dörr, T. Walter, M. Sahana, K. Brand, and L. Schultz, J. Magn. Magn. Mater. **242–245**, 447 (2002).
[27]M. Huijben, L. W. Martin, Y.-H. Chu, M. B. Holcomb, P. Yu, G. Rijnders, D. H. A. Blank, and R. Ramesh, Phys. Rev. B **78**, 094413 (2008).
[28]B. Kim, D. Kwon, J. H. Song, Y. Hikita, B. G. Kim, and H. Y. Hwang, Solid State Commun. **150**, 598 (2010).
[29]P. M. Leufke, A. K. Mishra, A. Beck, D. Wang, C. Kübel, R. Kruk, and H. Hahn, Thin Solid Films **520**, 5521 (2012).
[30]With a sensitivity of 10^{-8} emu, the SQUID magnetometer can detect $\approx 10^{12}\mu_B$; in a classic approximation this is equivalent to $\approx 10^{12}$ electrons.
[31]P. M. Leufke, R. Kruk, D. Wang, C. Kübel, and H. Hahn, AIP Advances **2**, 032184 (2012).
[32]N. Izyumskaya, Y. I. Alivov, S. J. Cho, H. Morkoç, H. Lee, and Y. S. Kang, Crit. Rev. Solid State Mater. Sci. **32**, 111 (2007).
[33]M. Nguyen, Ph.D. thesis, Universiteit Twente, 2010 (unpublished).
[34]J. F. Scott, L. Kammerdiner, M. Parris, S. Traynor, V. Ottenbacher, A. Shawabkeh, and W. F. Oliver, J. Appl. Phys. **64**, 787 (1988).
[35]P. K. Larsen, G. L. M. Kampschöer, M. J. E. Ulenaers, G. A. C. M. Spierings, and R. Cuppens, Appl. Phys. Lett. **59**, 611 (1991).
[36]J.-l. Chen, H.-m. Chen, and J. Y.-m. Lee, Appl. Phys. Lett. **69**, 4011 (1996).
[37]J. J. Lee, C. L. Thio, and S. B. Desu, J. Appl. Phys. **78**, 5073 (1995).
[38]M. Dawber, K. Rabe, and J. F. Scott, Rev. Mod. Phys. **77**, 1083 (2005).
[39]K. Rabe, M. Dawber, C. Lichtensteiger, C. Ahn, and J. Triscone, Physics Ferroelectrics **30**, 1 (2007).
[40]S. Dussan, A. Kumar, R. S. Katiyar, S. Priya, and J. F. Scott, J. Phys.: Condens. Matter **23**, 202203 (2011).
[41]B. Dabrowski, X. Xiong, Z. Bukowski, R. Dybzinski, P. W. Klamut, J. E. Siewenie, O. Chmaissem, J. Shaffer, C. W. Kimball, J. D. Jorgensen, and S. Short, Phys. Rev. B **60**, 7006 (1999).
[42]O. Chmaissem, B. Dabrowski, S. Kolesnik, J. Mais, J. D. Jorgensen, and S. Short, Phys. Rev. B **67**, 094431 (2003).
[43]F. S. Razavi, G. Gross, H.-U. Habermeier, O. Lebedev, S. Amelinckx, G. Van Tendeloo, and A. Vigliante, Appl. Phys. Lett. **76**, 155 (2000).
[44]A. Vigliante, U. Gebhardt, A. Rühm, P. Wochner, F. S. Razavi, and H. U. Habermeier, Europhys. Lett. **54**, 619 (2001).
[45]J. Zhang, H. Tanaka, T. Kanki, J.-H. Choi, and T. Kawai, Phys. Rev. B **64**, 184404 (2001).
[46]A. Arrott, Phys. Rev. **108**, 1394 (1957).
[47]For better comparability, both curves are centered with respect to the polarization and magnetization modulation and the latter axis is flipped. Centering of FE hystereses is a common practice, as the net polarization—i.e., the constant of current integration—is not well defined.
[48]L. L. Boyer, N. Velasquez, and J. T. Evans, Jpn. J. Appl. Phys. **36**, 5799 (1997).
[49]D. Damjanovic, Rep. Prog. Phys. **61**, 1267 (1998).
[50]S. Dong, X. Zhang, R. Yu, J.-M. Liu, and E. Dagotto, Phys. Rev. B **84**, 155117 (2011).
[51]H. Molegraaf, J. Hoffman, J. Stahn, and S. Gariglio, in THIOX Thin Films For Novel Oxide Devices, Final Meeting, Sestri Levante, Italy, 2008 (unpublished).
[52]C. A. F. Vaz, Y. Segal, J. Hoffman, F. J. Walker, and C. H. Ahn, J. Vac. Sci. Technol. B **28**, C5A6 (2010).
[53]Only half of the Mn moments align antiparallel, while the other half remain (unchanged) parallel to the external field: $0.5 \times 2 \times (-3.6\mu_B) = -3.6\mu_B$.
[54]H. Chen and S. Ismail-Beigi, Phys. Rev. B **86**, 024433 (2012).
[55]E. Dagotto, Phys. Rep. **344**, 1 (2001).
[56]A. Alberca, C. Munuera, J. Tornos, F. J. Mompean, N. Biskup, A. Ruiz, N. M. Nemes, A. de Andres, C. León, J. Santamaría, and M. García-Hernández, Phys. Rev. B **86**, 144416 (2012).